THE JOURNAL OF BIOLOGICAL CHEMISTRY
Vol. 278, No. 51, Issue of December 19, pp. 50985–50998, 2003
Printed in U.S.A.

Mechanism of Nicotinamide Inhibition and Transglycosidation by Sir2 Histone/Protein Deacetylases*

Received for publication, June 20, 2003, and in revised form, September 11, 2003
Published, JBC Papers in Press, September 30, 2003, DOI 10.1074/jbc.M306552200

Michael D. Jackson‡, Manning T. Schmidt‡, Norman J. Oppenheimer§, and John M. Denu‡¶

From the ‡Oregon Health and Sciences University, Department of Biochemistry and Molecular Biology, Portland, Oregon 97201-3089 and the §Department of Pharmaceutical Chemistry, University of California, San Francisco, California 94143-0446

Silent information regulator 2 (Sir2) enzymes catalyze NAD$^+$-dependent protein/histone deacetylation, where the acetyl group from the lysine ϵ-amino group is transferred to the ADP-ribose moiety of NAD$^+$, producing nicotinamide and the novel metabolite *O*-acetyl-ADP-ribose. Sir2 proteins have been shown to regulate gene silencing, metabolic enzymes, and life span. Recently, nicotinamide has been implicated as a direct negative regulator of cellular Sir2 function; however, the mechanism of nicotinamide inhibition was not established. Sir2 enzymes are multifunctional in that the deacetylase reaction involves the cleavage of the nicotinamide-ribosyl, cleavage of an amide bond, and transfer of the acetyl group ultimately to the 2′-ribose hydroxyl of ADP-ribose. Here we demonstrate that nicotinamide inhibition is the result of nicotinamide intercepting an ADP-ribosyl-enzyme-acetyl peptide intermediate with regeneration of NAD$^+$ (transglycosidation). The cellular implications are discussed. A variety of 3-substituted pyridines was found to be substrates for enzyme-catalyzed transglycosidation. A Brönsted plot of the data yielded a slope of +0.98, consistent with the development of a nearly full positive charge in the transition state, and with basicity of the attacking nucleophile as a strong predictor of reactivity. NAD$^+$ analogues including β-2′-deoxy-2′-fluororibo-NAD$^+$ and a His-to-Ala mutant were used to probe the mechanism of nicotinamide-ribosyl cleavage and acetyl group transfer. We demonstrate that nicotinamide-ribosyl cleavage is distinct from acetyl group transfer to the 2′-OH ribose. The observed enzyme-catalyzed formation of a labile 1′-acetylated-ADP-fluororibose intermediate using β-2′-deoxy-2′-fluororibo-NAD$^+$ supports a mechanism where, after nicotinamide-ribosyl cleavage, the carbonyl oxygen of acetylated substrate attacks the C-1′ ribose to form an initial iminium adduct.

The acetylation state of histones is intimately coupled to transcription, DNA repair, and replication and is governed by the competing enzymatic activities of histone acetyltransferases and histone deacetylases (reviewed in Refs. 1–3). Recently a new family of histone deacetylases has emerged and is referred to as the silent information regulator 2 (Sir2)[1] family of histone/protein deacetylases (reviewed in Refs. 4–6) or Sirtuins (7). This family is highly conserved from prokaryotes to humans (7), and there is evidence suggesting that the scope of Sir2 activity extends beyond histone deacetylation and involves other protein targets throughout the cell. In yeast, at least five Sir2-like proteins have been identified. The founding member, yeast Sir2 (ySir2), is required for all major silenced loci (reviewed in Ref. 4). A Sir2 homologue from *Salmonella enterica* was shown to up-regulate acetyl-CoA synthetase, through deacetylation of a critical lysine residue (8, 9). In humans, seven Sir2 homologues have been identified to date (7). Of these seven, human SIRT2 (hSIRT2) has been identified as a cytosolic protein (10) that deacetylates α-tubulin at lysine 40, both *in vitro* and *in vivo* (11). Recent work has also shown that hSIRT3 is localized to the mitochondria (12, 13). The nuclear Sir2 homologue, SIRT1, has been reported to regulate the p53 tumor suppressor by deacetylation, resulting in inhibition of the p53-dependent apoptotic pathway (14, 15).

Class 1 and 2 histone deacetylases catalyze the deacetylation of histones/proteins to generate free acetate and the deacetylated protein. Based on sequence homology to a metalloprotease-like enzyme from the hyperthermophilic bacterium *Aquifex aeolicus*, the mechanism involves activation of a water molecule by a zinc atom and two aspartate/histidine ion pairs in the active site (16). In contrast, Sir2-like enzymes, which constitute class 3 histone deacetylases, require NAD$^+$ for catalytic activity (17–20), and deacetylation of substrate is tightly coupled to the formation of a novel compound, *O*-acetyl-ADP-ribose (*O*AADPr) (18, 21). Based on several lines of evidence (22–24), the initial enzymatic product is 2′-*O*-acetyl-ADP-ribose (2′-*O*AADPr), which subsequently equilibrates with 3′-*O*-acetyl-ADP-ribose (3′-*O*AADPr) in solution through a nonenzymatic intramolecular transesterification reaction. Although the physiological function of *O*AADPr is unclear, microinjection of *O*AADPr results in a delay/block in oocyte maturation and in a delay/block of embryo cell division (25). Enzymatic activities that metabolize *O*AADPr in cell extracts have been described (26), providing further evidence for an important role in cell signaling or metabolism.

In yeast, several recent reports (17, 27–29) have implicated a

* This work was supported by National Institutes of Health Grant GM65386, American Cancer Society Grant RSG-01-029-01 (to J. M. D.), and by National Institutes of Health Post-doctoral Fellowship DK07680-12 (to M. D. J.). Portions of this work were presented as an abstract at the Experimental Biology 2003/American Society of Biochemistry and Molecular Biology national meeting, April 12, 2003, at San Diego, CA. The costs of publication of this article were defrayed in part by the payment of page charges. This article must therefore be hereby marked "*advertisement*" in accordance with 18 U.S.C. Section 1734 solely to indicate this fact.

¶ To whom correspondence should be addressed: Dept. of Biomolecular Chemistry, University of Wisconsin Medical School, 1300 University Ave., Madison, WI 53706. Tel.: 608-265-1859; Fax: 608-262-5253; E-mail: jmdenu@wisc.edu.

[1] The abbreviations used are: Sir2, silent information regulator 2; *O*AADPr, *O*-acetyl-ADP-ribose; HPLC, high pressure liquid chromatography; 2′-ribo-FNAD$^+$, 2′-deoxy-2′-fluoro-NAD$^+$; thio-NAD$^+$, thionicotinamide adenine dinucleotide; 3-Ac-PAD$^+$, 3-acetylpyridine adenine dinucleotide; 3-h-PAD$^+$, 3-hydroxypyridine adenine dinucleotide; wt, wild type; DTT, dithiothreitol; PBS, phosphate-buffered saline.

nuclear NAD^+ salvage pathway as a regulatory control point for ySir2. This salvage pathway conserves the pyridine ring of nicotinic acid or nicotinamide to regenerate β-NAD^+. Enzymes involved in this pathway influence ySir2-dependent gene silencing. Mutation of the NAD^+ salvage pathway gene *NPT1* (nicotinate phosphoribosyltransferase) results in silencing defects (29), whereas a single extra copy of the *PNC1* gene (nicotinamidase) is sufficient to increase ySir2-dependent silencing (28). Additional copies of *NPT1* led to increases in Sir2-dependent silencing and extended yeast replicative life span (27). How these pathway intermediates (nicotinamide metabolites) may affect directly Sir2-dependent deacetylation is not clear. However, nicotinamide has been suggested as an *in vivo* regulator of Sir2 function (6, 28), as physiological concentrations of nicotinamide inhibited ySir2, HST2, and human SIRT1 (hSIRT1) *in vitro* (28, 30), whereas exogenous nicotinamide added to yeast cells decreased gene silencing and accelerated aging (28), hallmarks of Sir2-deficient yeast. Although nicotinamide has been shown to be a potent inhibitor of several Sir2 homologues (28, 30), the mechanism of inhibition has not been established.

This paper focuses on three critical topics as follows: the mechanism of nicotinamide inhibition through the measurement of the efficiency by which nicotinamide/pyridine analogues can serve as substrates for transglycosidation; the nature of the transition state for transglycosidation; and the function of the 2′-hydroxyl of the nicotinamide ribose in the catalytic mechanism utilizing NAD^+ analogues and a catalytic mutant (His-to-Ala).

EXPERIMENTAL PROCEDURES

Reagents—All chemicals were of the highest purity commercially available, were purchased from Sigma, Aldrich, or Fisher, and were used without further purification. Synthetic 11-mer H3 peptide and acetylated H3 peptide (corresponding to the 10 amino acid residues surrounding lysine 14 of histone H3; H_2N-KSTGGK(Ac)APRKQ-$CONH_2$) were purchased from SynPep Corporation (Dublin, CA), ^{3}H-Labeled acetyl H3-peptide was prepared as reported previously (22). [*adenylate*-^{32}P]NAD^+ was purchased from ICN (Costa Mesa, CA). HST2 mutant H135A was a generous gift from Rolf Sternglanz (State University of New York, Stony Brook). 2′-Ribo-$FNAD^+$ and 2′-deoxy-ribo-NAD^+ were synthesized as described previously (31).

Expression and Purification of His-tagged HST2, HST2 Mutant H135A, hSIRT2, and ySir2—The procedure used in the expression and purification of histidine-tagged full-length HST2 has been reported previously (22) with only minor changes and was applied to the purification of the Sir2 enzymes. Fractions containing protein greater than 90% purity, based upon densitometry, were pooled, concentrated, and dialyzed in 50 mM Tris (pH 7.5, 37 °C) or PBS (pH 7.3), 10% glycerol, and 1 mM DTT. For yeast Sir2 (ySir2), 800 mM NaCl was also included in the final dialysis to prevent precipitation of protein. Enzyme concentrations were determined using the method of Bradford (32), and the stock solutions were stored at −25 °C until needed.

Charcoal Binding Assays—General enzymatic reactions contained ^{3}H-acetylated H3 peptide substrate, NAD^+, and a NAD^+-dependent Sir2-like class III protein/histone deacetylase to form the product ^{3}H-labeled *O*AADPr. To 70-μl reaction volumes was added 50 μl of charcoal slurry (1 volume of activated charcoal to 2 volumes of 2.0 M glycine buffer, pH 9.5) to terminate the reaction at the desired time points. The mixture was heated at 95 °C for 1 h and then centrifuged for 1 min at 7000 × *g*. A total of 90 μl of the supernatant was removed and added to 50 μl of fresh charcoal slurry, centrifuged again for 1 min, and 100 μl of the supernatant removed and added to a clean tube. This was centrifuged for 5 min, and 75 μl removed and quantified by liquid scintillation counting. This assay effectively measures the amount of ^{3}H-labeled *O*AADPr in the form of free acetate. Both *O*AADPr and acetylated H3 peptide bind to the activated charcoal. However, under these conditions the ^{3}H-labeled acetate from *O*AADPr is hydrolyzed and remains in the supernatant. Activated charcoal immediately stops the enzymatic reaction at all pH and temperature values tested. Heating and high pH is necessary only to hydrolyze acetate from *O*AADPr (data not shown). Amides, represented by unreacted peptide, are not hydrolyzed under these conditions (data not shown).

Nicotinamide Exchange Reactions—General exchange reactions for HST2, HST2 mutant H135A, hSIRT2, and ySir2 were performed in 50-μl volumes containing 500 μM NAD^+, 300 μM acetylated H3 peptide, 1 mM DTT, and buffer (PBS, pH 7.3, 37 °C, or 50 mM Tris-Cl, pH 7.5, 37 °C, as noted), 0.2 μM enzyme, and nicotinamide concentrations ranging from 3 μM to 1 mM containing [*carbonyl*-^{14}C]nicotinamide (Sigma N-2142, 52.8 mCi/mmol). Reactions were initiated via addition of enzyme, incubated at 37 °C for 5–8 min, and quenched with neat trifluoroacetic acid (to a final concentration of 1%). Linearity of rates was confirmed by measuring exchange over time courses up to 30 min. After quenching, 5 μl of each reaction was spotted to Whatman aluminum-backed Silica Gel TLC plates (Fisher) and placed in a development tank pre-equilibrated with 80:20 ethanol, 2.5 M ammonium acetate for 1 h (20). Plates were air-dried and exposed to a PhosphorImaging screen (Bio-Rad Molecular Imaging Screen-CS) for 24 h and then read with Bio-Rad GS-525 Molecular Imaging System and Molecular Analyst software (version 2.1.2). The percentage of nicotinamide exchanged was determined by measuring the densities of the [*carbonyl*-^{14}C]nicotinamide (R_f 0.80) and enzymatically created ^{14}C-labeled NAD^+ (R_f 0.27). Enzymatic exchange rates were fitted to the Michaelis-Menten equation (Equation 1) (Kaleidagraph, Synergy Software, Reading, PA). Reported values are the average of at least three independent experiments.

$$\nu_o = (k_{cat}\cdot[S])/(K_m + [S]) \quad \text{(Eq. 1)}$$

Nicotinamide Inhibition Curves—Nicotinamide inhibition reactions for both HST2 and hSIRT2 were performed in 80-μl volumes with 500 μM NAD^+, 300 μM ^{3}H-acetylated H3 peptide, 1 mM DTT, 50 mM Tris-Cl (pH 7.5, 37 °C), 0.5 μM enzyme, and nicotinamide concentrations ranging from 3 μM to 1 mM. Reactions were initiated by addition of enzyme, incubated at 37 °C for 5–8 min, and quenched with activated charcoal. Inhibition was determined by measuring the forward rate using the charcoal-binding assay (described above). Forward rates were fitted to Equation 2 using Kaleidagraph software. Reported values are the average of at least three independent experiments.

$$\nu_{app} = \nu_{max}(1 - ([I]/(K_{i(app)} + [I]))) \quad \text{(Eq. 2)}$$

Exchange Rates of Pyridine Derivatives for Use in Brönsted Analyses—Exchange reactions were performed in 70-μl volumes containing 500 μM NAD^+, 300 μM acetylated H3 peptide, 1 mM DTT, 50 mM Tris-Cl (pH 7.5, 37 °C), 0.2–1.0 μM HST2, and pyridine analogue concentrations ranging from 0.4 to 100 mM. The pH values of inhibitor stock solutions were checked for consistency. Reactions were initiated via addition of enzyme, incubated at 37 °C, and quenched with neat trifluoroacetic acid (to a final concentration of 1%). Quenched reactions were analyzed by HPLC. Two analytical C-18 columns (Vydac, 4.6 × 250 mm, 10 μm) were connected in tandem and run at 1 ml/min in 100% buffer A (0.05% trifluoroacetic acid/water) for 1 min and then ramped to 20% buffer B (0.02% trifluoroacetic acid/acetonitrile) for over 20 min. NAD^+ eluted from the column at 13 min, and the corresponding NAD^+ analogue made in the exchange reaction eluted 1–3 min later. Rates were determined by integrating the peaks and determining the amount of NAD^+ converted to its analogue. Reactions were quenched at 1, 2, and 3 min, and rates were determined by using linear least squares regression with Kaleidagraph software. Corresponding rates were then fitted to the Michaelis-Menten equation (Equation 1). The log of the rate for pyridine analogue exchange (V_{max}) was plotted against pK_a of the ring nitrogen of the pyridine analogue in the Brönsted plot and fitted using linear least squares regression (Kaleidagraph software).

TLC Conditions for the Analysis of Thionicotinamide and 3-Hydroxypyridine Inhibition Reactions—Inhibition reactions were performed in 60-μl volumes with 50 μM ^{32}P-labeled NAD^+ (ICN 37025, adenylate-^{32}P), 225 μM acetylated H3 peptide, 1 mM DTT, 50 mM inhibitor, 4.2 μM HST2, in 50 mM sodium phosphate buffer (pH 7.5, 37 °C). Nicotinamide was used as a control. Thionicotinamide reactions were run in 6.8% dimethyl sulfoxide (Me_2SO). Reactions were run for 10 min at 37 °C and quenched with neat trifluoroacetic acid to a final concentration of 1%. A total of 2 μl of each reaction was spotted onto Whatman aluminum-backed silica gel TLC plates and placed in a development tank pre-equilibrated with 70:30 ethanol, 2.5 M ammonium acetate for 4 h. The plate was air-dried, exposed to a β-imaging screen (Bio-Rad Molecular Imaging Screen-BI) for 3 h, and read as described above. Under these conditions NAD^+ has an R_f of 0.41, ADPr an R_f of 0.68, and *O*AADPr an R_f of 0.75.

Charcoal Binding Method Used for the Analysis of Pyridine Analogue Inhibition Reactions—Inhibition reactions were performed in 80-μl volumes with 50 μM NAD^+, 225 μM ^{3}H-acetylated H3 peptide, 1 mM DTT, 0.4 μM HST2, inhibitor concentrations spanning 1–30 mM, and in 50 mM

sodium phosphate buffer (pH 7.5, 37 °C). Reactions were initiated by addition of enzyme, incubated at 37 °C for 5–8 min, and quenched with activated charcoal. Inhibition was determined by measuring the forward rate using the charcoal-binding assay (described above). Reactions using thionicotinamide contained 6.8% Me_2SO and were compared with uninhibited reactions also in 6.8% Me_2SO as a control. Reported values are the average of at least three independent experiments.

Use of 2′-Deoxy-2′-fluororibo-NAD$^+$ and in Nicotinamide Exchange Reactions Catalyzed by HST2, HST2 Mutant H135A, and hSirT2—At fixed [nicotinamide], exchange reactions using 2′-ribo-FNAD$^+$ consisted of either 80–100 μM wt HST2 or HST2 mutant H135A or 50 μM hSIRT2, 800 μM 2′-ribo-FNAD$^+$, 300 μM AcH3 peptide, 50 μM nicotinamide (containing ^{14}C-labeled nicotinamide), 1 mM DTT, in phosphate-buffered saline (pH 7.3) at 37 °C. Reactions were initiated via the addition of enzyme and incubated for the indicated times at 37 °C. Reactions were quenched via the addition of neat trifluoroacetic acid to a final concentration of 1%, and 6-μl aliquots were analyzed by TLC as mentioned previously. To obtain the apparent V_{max} value for nicotinamide exchange with 2′-ribo-FNAD$^+$, reactions were carried out at 37 °C for 7.5 min and contained the following components: 7.8 μM hSIRT2 or 79 μM HST2, 1 mM DTT, 300 μM AcH3 peptide, 1.91 mM dFNAD in PBS (pH 7.3, 37 °C), and nicotinamide concentrations ranging from 50 to 2000 μM. Samples were incubated at 37 °C for 5 min prior to the addition of enzyme. Reactions were terminated via the addition of neat trifluoroacetic acid to a final concentration of 1% and were analyzed by HPLC and liquid scintillation counting as described before. Control reactions containing the varied range of [nicotinamide] but lacking enzyme were treated in the same manner to determine the extent of nonenzymatic incorporation of exogenous nicotinamide. The initial rate of nicotinamide exchange was determined by subtracting the amount of nicotinamide incorporation from the controls from the enzymatic reactions. The complete data set was then fitted to the Michaelis-Menten equation to obtain the apparent V_{max} for base exchange. The 2′-deoxyribo-NAD$^+$ analogue was analyzed similarly to that of 2′-deoxy-2′-fluororibo-NAD$^+$ except where noted in the legend of Fig. 5*B*.

Utilization of 2′-Deoxy-2′-fluororibo-NAD$^+$ as a Substrate in Forward Reactions Catalyzed by Wild-type HST2—Reactions were performed in triplicate and consisted of 100 μM HST2, 1 mM DTT, 500 μM [^{3}H]AcH3 peptide, 800 μM 2′-ribo-FNAD$^+$ in phosphate-buffered saline (pH 7.3, 37 °C). The reactions and controls were incubated at 37 °C from 0.25 to 30 min and quenched via the addition of charcoal slurry, either at pH 7 or pH 9.5. The transfer of [^{3}H]acetate from substrate to the ADP-ribose moiety of 2′-ribo-FNAD$^+$, in the form of free acetate, was determined using the charcoal-binding assay mentioned previously. Control reactions contained either no enzyme or 1% SDS and enzyme. Free acetate does not bind to charcoal at either pH 7 or pH 9.5, whereas [^{3}H]AcH3 peptide binds under both conditions and does not liberate free acetate, even under the pH 9.5 conditions. As with the normal product 2′-*O*AADPr generated by using NAD$^+$, the observed acetylated intermediate with 2′-ribo-FNAD$^+$ was measured as free acetate production under hydrolytic quenching. Under nonhydrolytic quenching (pH 7), this product bound to activated charcoal.

Enzymatic Synthesis of [carbonyl-^{14}C]2′-ribo-FNAD$^+$—A single reaction (1 ml) containing 100 μM HST2, 1 mM DTT, 500 μM acetylated H3 peptide, 800 μM 2′-ribo-FNAD$^+$, and 100 μM [*carbamoyl*-^{14}C]nicotinamide in PBS (pH 7.3, 37 °C) was incubated at 37 °C for 30 min. The reaction was terminated by the addition of neat trifluoroacetic acid to a final concentration of 1%, and the [*carbonyl*-^{14}C]2′-FNAD$^+$ was purified by HPLC as described previously (22). The peak corresponding to 2′-FNAD$^+$ was collected, lyophilized, and suspended in a small volume (100 μl) of water. The concentration of [*carbonyl*-^{14}C]2′-FNAD$^+$ was determined spectrophotometrically using the extinction coefficient of 18.1 mM^{-1} cm^{-1} at 260 nm.

Determination of the Rate of Nicotinamide Release Using 2′-ribo-FNAD$^+$ and Wild-type HST2—Reactions were performed in duplicate and consisted of 80 μM HST2, 1 mM DTT, 500 μM AcH3 peptide, 800 μM 2′-ribo-FNAD$^+$ (labeled with [^{14}C]nicotinamide) in phosphate-buffered saline (pH 7.3, 37 °C). The reactions were incubated at 37 °C for the indicated time intervals and quenched via the addition of neat trifluoroacetic acid to a final concentration of 1%. Reactions were then analyzed by HPLC as described previously. The extent of nicotinamide liberation was determined by liquid scintillation counting and correlated to nicotinamide concentrations in the reactions. Linear data points were plotted using linear least squares, and the rate of nicotinamide release was calculated from the slope of the graph.

RESULTS

The following experiments have focused on the following three topics: the origin of nicotinamide noncompetitive inhibition; the nature of the transition state for formation of the nicotinamide-ribosyl bond; and the utilization of NAD$^+$ analogues to probe the mechanism of deacetylation catalyzed by Sir2-like enzymes.

Mechanism of Nicotinamide Inhibition—Several recent reports (17, 27, 28) have implicated a nuclear NAD$^+$ salvage pathway in the regulation of ySir2 function. Nicotinamide, a key salvage intermediate, has been suggested as an *in vivo* negative regulator of ySir2 activity (6, 28). Nicotinamide has been shown to be an effective noncompetitive inhibitor *versus* NAD$^+$ (28, 30) and *versus* acetylated substrate for the Sir2-like enzymes.[2] The physical basis for this potent inhibition of Sir2 was not obvious. One study suggested that nicotinamide acts as a classical dead-end inhibitor by binding to an alternative site on the enzyme surface, in close proximity to the active site (28). The observation of a small pocket described as site C in the x-ray structure led to speculation that this could be the putative binding site, although no nicotinamide moiety, either free or as NAD$^+$, has been observed in any of the reported structures (24, 33). Alternatively, inhibition could occur via the mechanism as observed for CD38 (34), namely the reaction of exogenous nicotinamide with an ADP-ribose-Sir2 intermediate that resynthesizes NAD$^+$, *i.e.* transglycosidation, thus partitioning the intermediate between reversal to starting substrate or continuation to product (30).

To examine whether transglycosidation can account for the observed nicotinamide inhibition, we have investigated in detail the ability of Sir2 homologues to catalyze a nicotinamide:NAD$^+$ exchange (20, 30). Sir2-catalyzed transglycosidation can be followed by measuring the incorporation of exogenous ^{14}C-labeled nicotinamide into NAD$^+$ in the presence of enzyme and acetylated substrate. We first examined the relationship between nicotinamide exchange and inhibition of the forward reaction by using yeast HST2 and human SIRT2 (hSIRT2). The nicotinamide exchange rate, *i.e.* the rate of ^{14}C label from exogenous nicotinamide appearing in NAD$^+$, was determined under saturating conditions of NAD$^+$ and acetylated H3 peptide, and increasing concentrations of nicotinamide as described under "Experimental Procedures." As depicted in Fig. 1, both HST2 (Fig. 1*A*) and hSIRT2 (Fig. 1*B*) showed rapid nicotinamide exchange rates (3.3 ± 0.2 and 2.4 ± 0.3 s^{-1}, respectively) that were saturable with respect to nicotinamide. These values establish that the transglycosidation represents a kinetically competent reaction, because the k_{cat} value for the forward deacetylation reaction is ~0.2 s^{-1} (18). Furthermore, the reaction was dependent on the presence of the full ternary complex of NAD$^+$, acetylated protein, and Sir2. No detectable exchange occurred with NAD$^+$ and enzyme or with NAD$^+$, enzyme, and unacetylated peptide. The apparent K_m values for the nicotinamide exchange reaction were 446 ± 18 and 37.8 ± 4.1 μM for HST2 and hSIRT2, respectively. Nicotinamide inhibition on the rate of the forward reaction (*O*AADPr production) was inversely proportional to the exchange rate (see Fig. 1). The inhibition data were fitted to Equation 2, which describes how the initial velocity would be affected as a function of nicotinamide, and provides a kinetic-derived parameter for the concentration of nicotinamide at 50% inhibition. This apparent K_i value is a weighted average of the noncompetitive inhibition kinetic constants of K_{ii} and K_{is} and depends

[2] M. T. Borra, M. R. Langer, J. T. Slama, and J. M. Denu, manuscript in preparation.

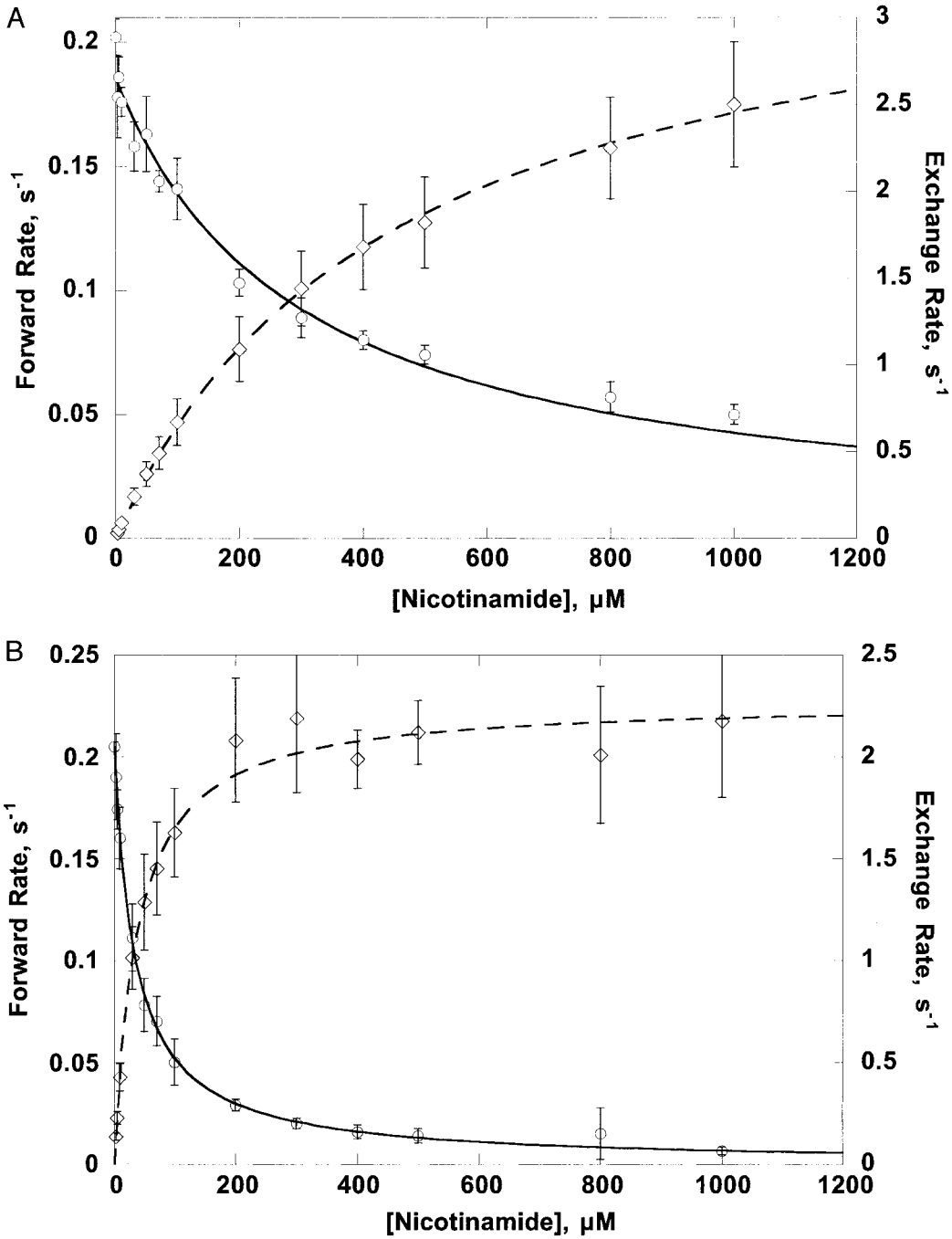

FIG. 1. **Nicotinamide base exchange (transglycosidation) correlates with nicotinamide inhibition of the deacetylation.** *A*, nicotinamide exchange (*dotted lines*) and inhibition (*solid lines*) as observed using the yeast Sir2 homologue HST2. *B*, nicotinamide exchange and inhibition as observed using human SIRT2. Assays consisted of 0.2 (exchange reaction) or 0.5 μM (deacetylase reaction) HST2 or hSIRT2, 500 μM β-NAD$^+$, 1 mM DTT, and 300 μM AcH3 peptide in 50 mM Tris-Cl, pH 7.5, 37 °C. Reactions were incubated at 37 °C (50 mM Tris, pH 7.5) for 5–8 min and terminated either by the addition of neat trifluoroacetic acid to a final concentration of 1% for the exchange assays, or addition of a 2 M glycine (pH 9.5)/charcoal slurry for the inhibition assays. Nicotinamide exchange was determined by analysis of the reaction mixture using TLC (80:20 EtOH, 2.5 M NH_4OAc) and PhosphorImaging to determine the extent of incorporation of [*carbonyl*-^{14}C]nicotinamide into β-NAD$^+$. Product inhibition was determined by monitoring the extent of product formation (*O*-acetyl-ADP-ribose) via the charcoal assay using ^{3}H-labeled AcH3 peptide.

partly on initial NAD$^+$ concentration. At saturating concentrations of NAD$^+$ (500 μM), the apparent K_i of hSIRT2 for nicotinamide was 33.9 ± 1.3 μM. This is in agreement with the reported value of $IC_{50} < 50$ μM for hSIRT1 (28) and of the hSIRT2 kinetic constants[2] for nicotinamide against NAD$^+$, where K_{is} = 14.6 ± 2.2 μM and K_{ii} = 60.5 ± 12.1 μM were observed. The K_{is} and the K_{ii} refer to the noncompetitive inhibition constants determined from the separate inhibitory effects on the slope ($1/V/K$) and the intercept ($1/V_{max}$) from a Lineweaver-Burk analysis. For HST2, we determined an apparent K_i of 298 ± 25 μM, which is in close agreement with an approximation (207 ± 4 μM) we derived from the data presented by Landry *et al.* (30).[3]

[3] This approximation was made by refitting the data points for the nicotinamide inhibition curve at 500 μM NAD$^+$, presented in a Lineweaver-Burk plot, into Equation 2.

TABLE I

Inhibitory effects of pyridine analogs on the catalyzed formation of O-acetyl-ADP-ribose

All reactions were carried out in 50 mM sodium phosphate buffer, pH 7.5, at 37 °C, 225 μM acetylated H3 peptide, 1 mM DTT, 50 μM β-NAD^+, and 0.4 μM HST2. Values are an average of three or more independent experiments. Values in parentheses indicate the concentration of compound tested.

Entry No.	Structure	Name	% Inhibition at Low Conc.	% Inhibition at High Conc.	pKa of Nitrogen[a]
1	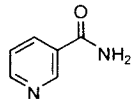	Nicotinamide	54.1 ± 0.7 (0.1 mM)	95.0 ± 0.7 (1.5 mM)	3.54 ± 0.11
2	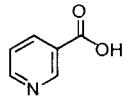	Nicotinic Acid	2.1 ± 1.8 (1 mM)	18.3 ± 3.3 (15 mM)	2.17 ± 0.20
3	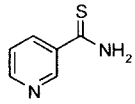	Thionicotinamide[b]	16.2 ± 1.8 (1 mM)	58.3 ± 0.5 (15 mM)	3.71 ± 0.11
4	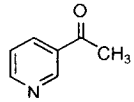	3-Aceytlpyridine	7.1 ± 2.0 (5 mM)	16.8 ± 2.1 (30 mM)	3.43 ± 0.20
5	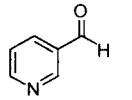	3-Pyridine-carboxyaldehyde	< 2% (5 mM)	10.6 ± 1.4 (30 mM)	3.43 ± 0.20
6	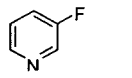	3-Fluoropyridine	N/D[c] (5 mM)	< 2% (30 mM)	2.81 ± 0.20
7	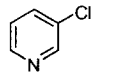	3-Chloropyridine	4.0 ± 1.9 (5 mM)	9.0 ± 1.3 (30 mM)	2.95 ± 0.20
8	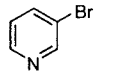	3-Bromopyridine	5.6 ± 4.1 (5 mM)	19.1 ± 0.8 (30 mM)	2.87 ± 0.20
9	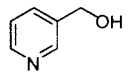	3-Pyridinemethanol	9.3 ± 1.0 (5 mM)	22.5 ± 1.9 (30 mM)	4.74 ± 0.20
10	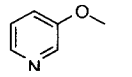	3-Methoxypyridine	5.3 ± 2.1 (5 mM)	10.8 ± 1.6 (30 mM)	4.67 ± 0.20
11	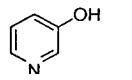	3-Hydroxypyridine	34.5 ± 1.2 (1 mM)	83.9 ± 2.0 (15 mM)	4.86 ± 0.20
12	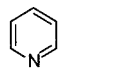	Pyridine	< 2% (5 mM)	6.4 ± 2.4 (30 mM)	5.32 ± 0.20

[a] pK_a values cited from Chemical Abstracts and were calculated from ACD (Advanced Chemistry Development) Software Solaris Version 4.67.
[b] Thionicotinamide reactions were performed in 6.8% Me_2SO (final concentration) and compared with the uninhibited forward reaction in 6.8% Me_2SO.
[c] Not detected.

Use of Nicotinamide Analogues to Probe the Nature of the Nicotinamide-binding Site and Reactivity of an Enzyme-ADP-ribose-like Intermediate—To probe further the mechanism of nicotinamide inhibition, a variety of nicotinamide analogues were evaluated. These 3-substituted pyridines were selected based upon the nature of the functional group and the nucleophilicity of the base nitrogen. Table I lists the 12 pyridine derivatives tested in this study. To provide an initial assessment of the binding affinity and reactivity of each derivative, the ability to inhibit the deacetylation rate at two concentra-

tions of each derivative was determined (Table I). As with nicotinamide, the level of inhibition should be dictated by both the nucleophilicity and the differential binding due to the various size and physical properties, *e.g.* hydrogen-bonding capabilities, of the functional group at C-3 of pyridine.

For our study, pyridine derivatives were categorized based on the presence of a carbonyl or sulfonyl carbon (entries 2–5), electron-withdrawing substituents (entries 6–8), or electron-donating groups (entries 9–11) at the C-3 position of pyridine. Thionicotinamide was the best nicotinamide derivative tested, showing inhibition that was 33-fold lower than that observed for nicotinamide. However, the strongest overall pyridine inhibitor was found to be 3-hydroxypyridine (entry 11, ~16-fold lower inhibition), indicating that activation of the ring nitrogen by a strong electron-donating group can partially offset the lack of potential binding interactions when the functional group at C-3 is something other than a primary amide. Another example where activation of the ring nitrogen is dependent upon the electronegativity of the functional group is found in entries 6–8. As the electronegativity of the functional group decreases, the inhibitory effect of the compound on the forward reaction increases (R = F (entry 6), no detectable inhibition; R = Cl (entry 7), 676-fold lower inhibition than nicotinamide; R = Br (entry 8), 480-fold lower inhibition than nicotinamide).

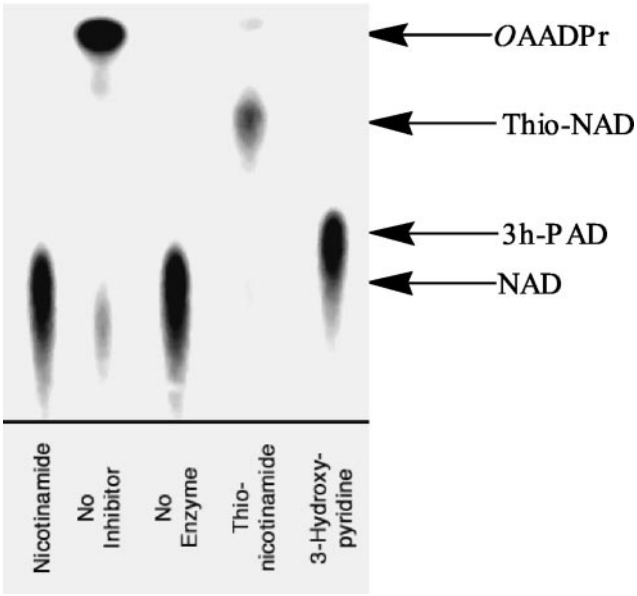

FIG. 2. **Evidence for enzyme-catalyzed formation of NAD^+ analogues using pyridine derivatives.** TLC analysis of reactions containing 50 μM ^{32}P-labeled NAD^+, 225 μM acetylated H3 peptide, 4.2 μM HST2, and 50 mM inhibitor. Detailed conditions of the TLC are described under "Experimental Procedures." NAD^+ exhibited an R_f of 0.41 and *O*AADPr an R_f of 0.75. The new compound in the *4th lane* (R_f of 0.64) was identified as thionicotinamide adenine dinucleotide by mass spectrometry. The *5th lane* also exhibited a new compound having an R_f of 0.49 and was identified as 3-hydroxypyridine adenine dinucleotide by mass spectrometry.

Based on our observations that a variety of pyridine derivatives inhibit the forward reaction, we examined whether the inhibitory effects were indeed due to an enzyme-catalyzed condensation of the base (transglycosidation) with an ADP-ribose-like intermediate to generate a unique dinucleotide substrate. To ascertain formation of the unique dinucleotide substrates, the base exchange reactions (with HST2) were performed with ^{32}P-NAD^+, AcH3 peptide, and 50 mM of either 3-hydroxypyridine or thionicotinamide and analyzed by TLC as described under "Experimental Procedures." As Fig. 2 illustrates, inclusion of either 3-hydroxypyridine or thionicotinamide resulted in the formation of new compounds having retention factors (R_f) of 0.49 and 0.64, respectively, concomitant with the disappearance of NAD^+ (R_f = 0.27). For structural identification of the compounds, reaction components were purified by HPLC, lyophilized, and analyzed by mass spectrometry, which identified the formation of 3-h-PAD^+ (m/z = 637 (M^+)) and thio-NAD^+ (m/z = 680 (M^+)). It should be noted that in the presence of these nicotinamide analogues, negligible formation of *O*AADPr was observed, and nearly all of the NAD^+ was converted to the corresponding NAD^+ analogue.

To determine whether the transglycosidation reactions observed with HST2 might be representative throughout the Sir2 class of deacetylases, we tested 3-hydroxypyridine and thionicotinamide with the Sir2 homologues hSIRT2 and yeast Sir2 (ySir2). TLC analysis of the exchange reactions showed the formation of 3-h-PAD^+ and thio-NAD^+, with minimal formation of *O*AADPr. With respect to inhibition of the forward reaction, all bases tested (3-hydroxypyridine, thionicotinamide, nicotinamide, and nicotinic acid) were in agreement with the trends observed with HST2 (data not shown).

With nicotinamide/pyridine inhibition established to be the result of the base condensing with an ADP-ribose-enzyme intermediate, we utilized this reaction to probe the nature of the

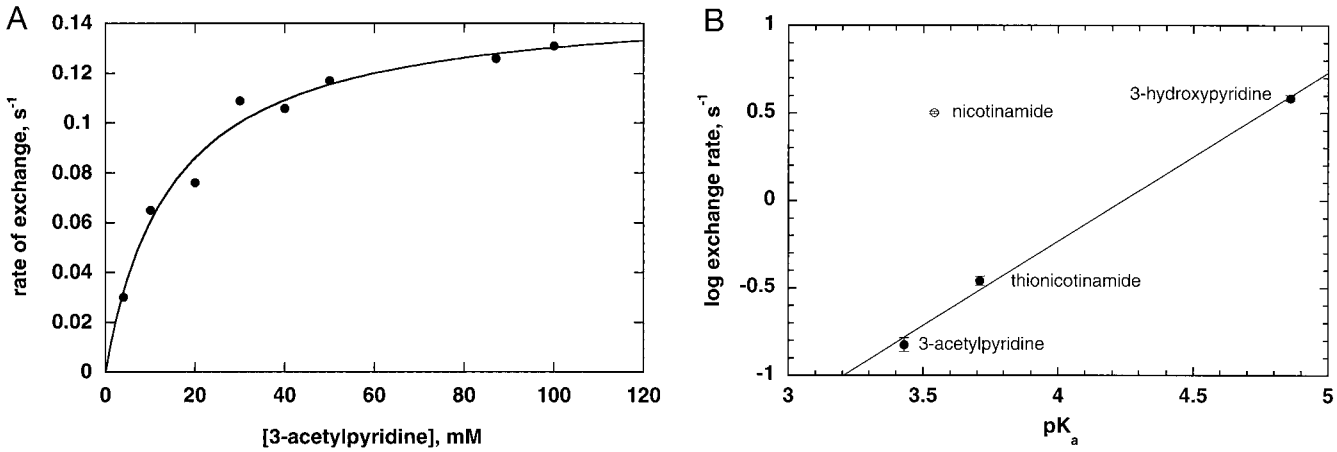

FIG. 3. **Determining the V_{max} for base exchange using pyridine derivatives and subsequent Brönsted analysis.** *A*, Michaelis-Menten plot of the exchange rate for 3-acetylpyridine. Reactions were performed in 50 mM Tris (pH 7.5, 37 °C), containing 300 μM AcH3, 500 μM NAD^+, 1 mM DTT, and 0.2–1.0 μM HST2. Rates were determined by HPLC as described under "Experimental Procedures." *B*, Brönsted analysis of the bases tested showing the log of the rate for pyridine analogue exchange (V_{max}) *versus* pK_a value of the ring nitrogen. The linear least squares fit yielded a slope of +0.98. Nicotinamide was excluded from the fit. Exchange rates were determined from saturation curves for each exchange reaction and are the average of at least three independent experiments (as represented in *A*).

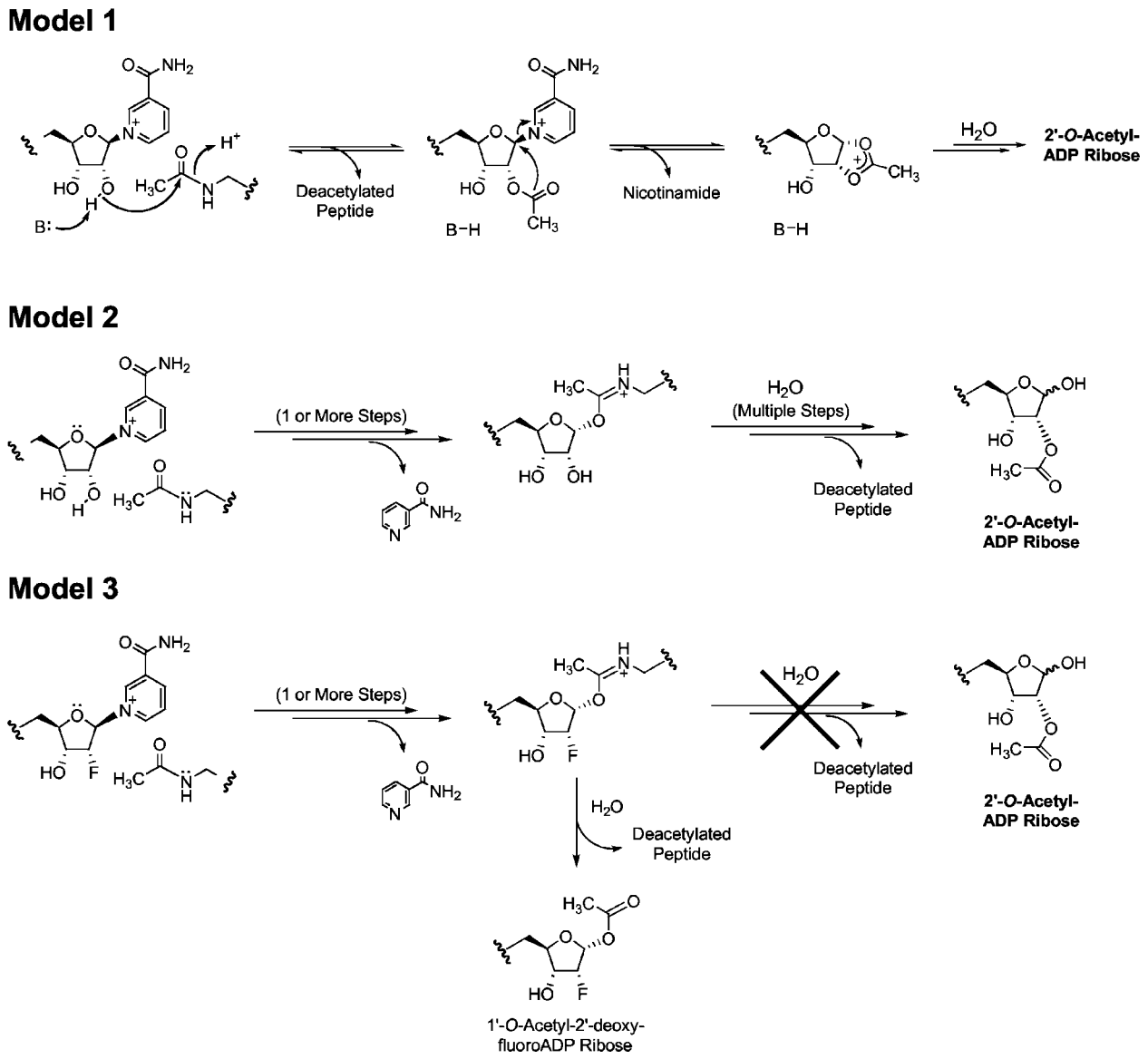

SCHEME 1. **General models (*models 1–3*) for the formation of 2′-*O*-acetyl-ADP-ribose or 1′-*O*-acetyl-2′-deoxy-fluoro-ADP-ribose from NAD$^+$ or 2′-ribo-FNAD$^+$ and acetylated substrate.**

transition state by performing a Brönsted analysis using several of the most effective inhibitors (Table I). The maximum exchange velocities (V_{max}) for 3-hydroxypyridine, 3-acetylpyridine, and thionicotinamide were obtained under saturating conditions of NAD$^+$ and acetylated peptide and varied [base] (Fig. 3*A*), and were plotted as a function of the ring nitrogen pK_a value (Fig. 3*B*). The use of the V_{max} for transglycosidation for each base eliminates the effects due to ground state binding affinity. This analysis yielded a slope of +0.98, consistent with the development of a nearly full positive charge in the transition state, and with basicity of the attacking nucleophile as a strong predictor of reactivity. Interestingly, nicotinamide does not fall on the Brönsted line of 3-substituted pyridines (Fig. 3*B*), indicating that additional considerations play a role in the selectivity for the base.

Use of 2′-Deoxy-2′-fluororibo-NAD$^+$ to Probe the Catalytic Mechanism of Sir2 Deacetylases—NAD$^+$ analogues containing 2′-deoxy-2′-*X*-substituted nicotinamide ribosides and arabinosides have been used to probe the steric H-bonding and inductive effects of the 2′-substituent on the chemical mechanism of CD38/NAD$^+$ glycohydrolases (35–37). The CD38 enzymes generate an activated ADP-ribose intermediate that can partition between reaction with solvent (NAD$^+$ glycohydrolase activity), reaction with the adenine moiety to form cyclic ADR-ribose (cyclization), and with exogenous nicotinamide or other bases to reform NAD$^+$ or NAD$^+$ analogues (transglycosidation).

Sir2-like enzymes catalyze a similarly complex series of reactions including both a transglycosidation reaction with exogenous nicotinamide and the deacetylation reaction of the peptide with the ultimate transfer of the acetyl group to the 2′-hydroxyl of the resulting ADP-ribose. Here we used the NAD$^+$ analogue 2′-deoxy-2′-fluoro-NAD$^+$ (2′-ribo-FNAD$^+$) to investigate the mechanism of glycosidic bond cleavage and acetyl transfer.

Two general models of the reaction mechanism have been proposed as outlined in Scheme 1 (models 1 and 2). Model 1 involves an initial attack of the 2′-hydroxyl to generate a bound 2′-*O*Ac-NAD$^+$ intermediate followed by attack of the acetyl carbonyl and expulsion of the nicotinamide moiety to form an initial 1′-2′-cyclic intermediate. Final hydrolysis of the 1′-2′-cyclic intermediate would generate the reaction product. Model 2 proposes an initial cleavage of the nicotinamide ribosyl bond and generation an activated ADPr intermediate (iminium)

through attack of the acetyl carbonyl. This iminium intermediate could either be hydrolyzed to form an enzyme-bound 1′-*O*AADPr intermediate or react with an activated hydroxyl group at C-2′, followed by hydrolysis to generate the ultimate product 2′-OAADPr (discussed below).

As shown in model 3 of Scheme 1, these two general mechanisms are readily distinguished through the use of the NAD^+ analogue, 2′-ribo-$FNAD^+$. If the catalytic mechanism involves an initial attack by the 2′-hydroxyl (as in model 1), then the replacement of the 2′-OH by fluorine should lead to a complete inhibition of both transglycosidation and acetyl group transfer. Alternatively, if the catalytic mechanism involves an initial cleavage of the nicotinamide-ribosyl bond with formation of an activated ADP-ribosyl intermediate, then replacement of the 2′-OH by fluorine should permit transglycosidation, but perhaps at a decreased rate due to its inductive effect (38) (Scheme 1, model 3). Furthermore, if the acetyl group condenses with the anomeric position at C-1′, then the absence of the 2′-OH should lead to trapping of an imine intermediate and the possible generation of 1′-*O*-aceytl-2′-deoxy-2′-fluoro-ADP-ribose and deacetylated substrate as the enzymatic products (Scheme 1, model 3). Previously, the formation of α-1′-*O*-acetyl-ADPr had not been observed either enzymatically or nonenzymatically via an intramolecular transesterification reaction (22, 23). This could be due to the rapid transfer of the acetyl group to the 2′-OH that is strongly favored both sterically and thermodynamically.

To address the chemical mechanism and to investigate the role of the 2′-OH during acetyl group transfer, acetylated peptide, 2′-ribo-$FNAD^+$, and enzyme were reacted and the products analyzed. Specifically, we examined whether acetyl group transfer to the anomeric carbon can occur in the absence of a C-2′ acceptor. The enzyme assays were performed under saturating ^{3}H-labeled, acetylated H3 peptide (500 μM) and 2′-ribo-$FNAD^+$ at 800 μM. Initially, reactions were terminated at 30 min, and deacetylation of peptide was monitored using the charcoal binding method as described under "Experimental Procedures." A low but measurable amount of free acetate was found using this assay (Fig. 4*A*, *bar 1*); however, free acetate was not the initial species produced by the enzymatic reaction. Instead, a relatively labile, acetylated intermediate was formed, which bound to activated charcoal under mild conditions (pH 7) (Fig. 4*A*, *bar 4*) but was hydrolyzed to free acetate at pH 9.5 (Fig. 4*A*, *bar 1*). This behavior is similar to that typically observed with the normal products of the reaction, 2′- and 3′-*O*AADPr, when NAD^+ is used as the co-enzyme. Control reactions indicated that the liberation of acetate was not due to solution hydrolysis of the acetylated peptide substrate (Fig. 4*A*, *bars 2* and *3*). A time-dependent generation of the enzymatic product was observed using acetylated H3 peptide (500 μM), 2′-ribo-$FNAD^+$ (800 μM), and 100 μM HST2 (Fig. 4*A*, *inset*). After 30 min, the lack of additional acetate formation was attributable to loss in enzymatic activity under these conditions (37 °C), which is also observed with NAD^+. From the initial rate of acetate formation (Fig. 4*A*, *inset*), an apparent first-order rate of 1.6×10^{-4} s^{-1} was determined. To demonstrate that indeed the glycosidic bond of 2′-ribo-$FNAD^+$ was being cleaved by HST2 in the presence of acetylated peptide, the generation of free nicotinamide was measured (Fig. 4*B*). The initial rate for nicotinamide liberation was 1.2×10^{-4} s^{-1} (Fig. 4*B*), similar to the rate determined for the acetyl transfer.

To provide additional evidence that 2′-ribo-$FNAD^+$ binds to Sir2 enzymes, an apparent K_i for 2′-ribo-$FNAD^+$ was determined by employing 2′-ribo-$FNAD^+$ as an inhibitor against the NAD^+-dependent HST2 reaction. Under saturating concentrations of acetylated H3 peptide (300 μM), the apparent rates of *O*AADPr formation at four different 2′-ribo-$FNAD^+$ concentrations were measured, and the apparent K_i of 590 ± 160 μM for 2′-ribo-$FNAD^+$ was calculated.

Collectively, these experiments demonstrate that 2′-ribo-$FNAD^+$ binds and reacts with Sir2 enzymes to generate an aborted intermediate, consistent with an iminium at the C-1′ formed between the two substrates. Also, the 2′-OH is not required to form this initial intermediate.

β-2′-Deoxy-2′-Fluororibo-NAD^+ Supports Enzyme-catalyzed Transglycosidation—To provide chemical evidence that nicotinamide-ribosyl cleavage and acetyl transfer to the 2′-OH occur as distinct catalytic steps in the reaction, the nicotinamide exchange reaction was investigated using yeast HST2 and hSIRT2 with 2′-ribo-$FNAD^+$ as the coenzyme. As shown in Table II, 2′-ribo-$FNAD^+$ can function as a substrate for the enzyme-catalyzed nicotinamide exchange reaction. Exchange rates were determined at fixed [2′-ribo-$FNAD^+$] and increasing concentrations of nicotinamide (50–2000 μM). The resulting data were fitted to the Michaelis-Menten equation to obtain the apparent maximal rate of exchange (Fig. 5*A* and Table II), yielding rates of 0.016 and 0.002 s^{-1} for HST2 and hSIRT2, respectively. The rates with 2′-ribo-$FNAD^+$ are ~200- and 1200-fold slower than the exchange rates determined with NAD^+ under similar conditions (Table II). The calculated rates were completely dependent on enzyme and required the presence of acetylated peptide. Due to the inductive effects of the fluorine, nonenzymatic hydrolysis of 2′-ribo-$FNAD^+$ is 56-fold slower than NAD^+ (38). Here the enzyme-catalyzed rate differences between NAD^+ and 2′-ribo-$FNAD^+$ fall between the values observed previously for the solution (56-fold) and CD38-catalyzed hydrolysis (10^5-fold) of the nicotinamide-ribosyl bond (38).

To address whether the inductive effect of 2′-ribo-$FNAD^+$ alone could account for the low nicotinamide exchange rates, we attempted to measure exchange rates with 2′-deoxy-ribo-NAD^+ ($dNAD^+$), where the 2′-OH hydroxyl is replaced by a hydrogen. The analogue 2′-deoxy-ribo-NAD^+ is much less stable than NAD^+ or 2′-ribo $FNAD^+$ (38), so the background hydrolysis is significant, and obtaining very accurate values for the nicotinamide exchange is more problematic. By taking into account the background hydrolysis of $dNAD^+$ to nicotinamide and ADP-deoxyribose, which is a competing reaction *versus* the enzyme-catalyzed nicotinamide exchange, we observed the time-dependent nicotinamide exchange by HST2, with an initial rate of 2×10^{-4} s^{-1} at 25 °C (Fig. 5*B*). Under similar conditions with HST2, 2′-ribo-$FNAD^+$ gave an exchange rate of 8×10^{-5} s^{-1}, or 2.5-fold lower. The observation that 2′-ribo-$FNAD^+$ and $dNAD^+$ yielded similar but low rates of exchange suggests that the inductive effect of 2′-ribo-$FNAD^+$ may not account fully for its low transglycosidation rate. Instead, the data suggest that although these derivatives can support transglycosidation, simply lacking the 2′-OH can adversely affect the efficiency of the transglycosidation reaction.

Together, these data suggest that the first step in the catalytic mechanism for deacetylation does not involve the initial attack of the 2′-OH of NAD^+ (Scheme 1, model 1), but rather involves the cleavage of the glycosidic bond between the ribose and nicotinamide to form an intermediate species that can perform transglycosidation (Scheme 1, model 2), regardless of the nature of the group at C-2′.

Role of a Conserved Histidine in the Transglycosidation and Acetyl Group Transfer Reactions—The catalytic events leading to acetyl group transfer from peptide to NAD^+ were investigated using the catalytic mutant of HST2, H135A. The histidine residue at position 135 of HST2 is an invariant residue found in all Sir2 enzymes. From the reported crystal structures of Sir2 homologues (24, 33, 39), it has been proposed that this

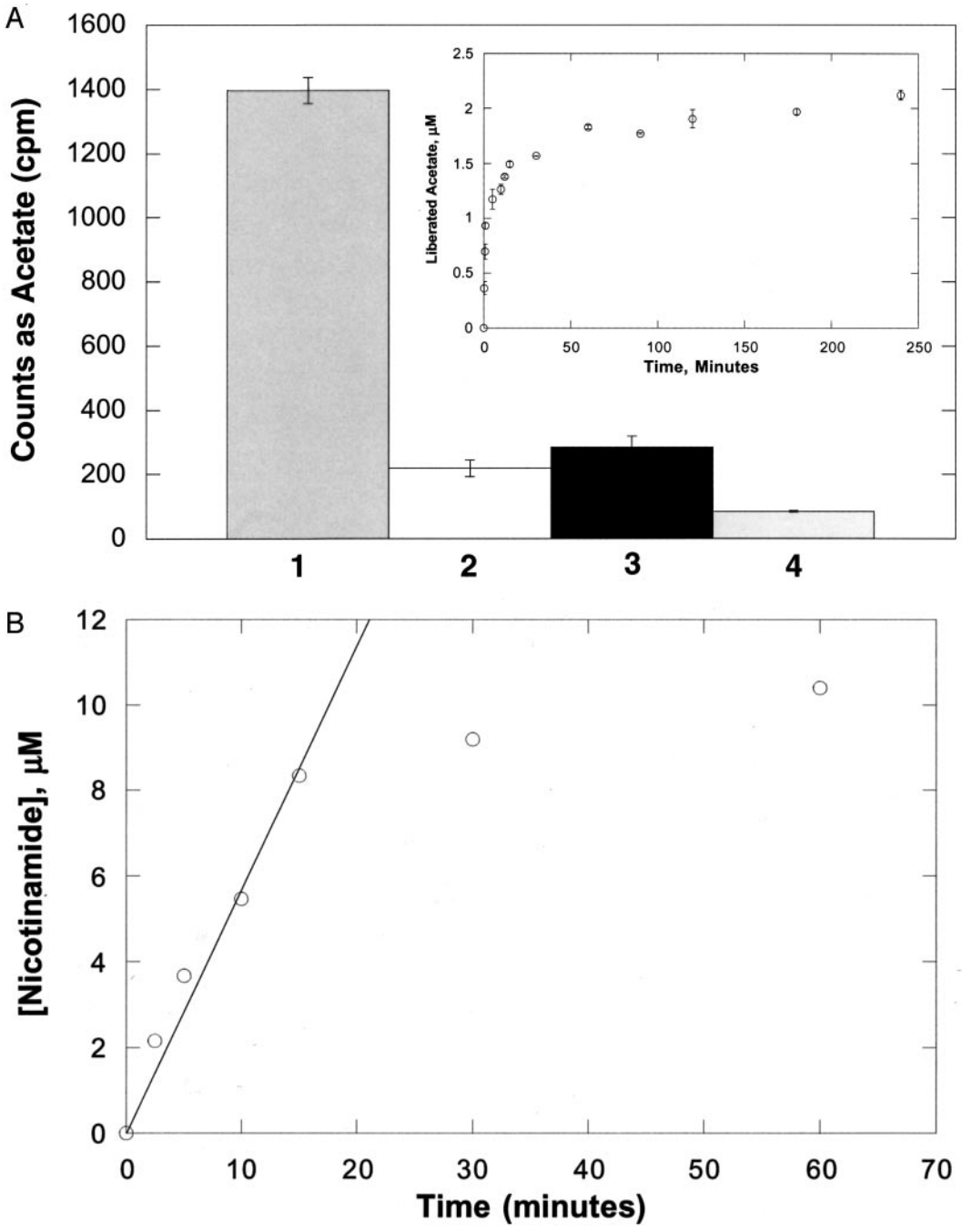

FIG. 4. **Use of the NAD$^+$ analogue 2′-deoxy-2′-fluoro-NAD$^+$ in HST2-catalyzed reactions.** *A*, HST2-catalyzed acetyl transfer. *Bar 1*, detection of acetate released when reactions were quenched under hydrolytic conditions (pH 9.5). Reactions (30 min, pH 7.3, and 37 °C) contained 100 μM HST2, 500 μM ^{3}H-labeled acetylated H3 peptide, and 800 μM 2′-ribo-FNAD$^+$ and were performed in triplicate. Control reactions contained either no enzyme (*bar 2*), 1% SDS prior to the addition of enzyme (*bar 3*), or the reaction quenched with charcoal slurry containing 2 M glycine (pH 7) to demonstrate charcoal adsorption of acetylated intermediate under nonhydrolytic conditions (*bar 4*). *Inset* shows the production of free acetate over time when 2′-ribo-FNAD$^+$ (800 μM) was used as the co-enzyme. *B*, liberation of free nicotinamide using 2′-ribo-FNAD$^+$. Reaction conditions were identical to those described for acetate formation with the exception that 80 μM HST2 was used. Reactions were worked up as described under "Experimental Procedures" and analyzed by liquid scintillation counting to determine the extent of nicotinamide formation.

conserved histidine activates the 2′-hydroxyl group of NAD$^+$ through a network of hydrogen bonds in order to facilitate transfer of the acetyl group of substrate (peptide or protein) to the 2′-hydroxyl group of ADP-ribose (22–24, 33). Although this residue has been shown to be mutationally sensitive (33), the apparent k_{cat} for base exchange and turnover had not been determined. Characterization of the mutant under saturating conditions of NAD$^+$ and acetylated peptide revealed an apparent k_{cat} value of 0.002 s^{-1}, ~100-fold lower than wild-type enzyme (0.21 s^{-1}). The nicotinamide exchange rate for H135A, however, was 0.12 s^{-1}, only 3-fold lower than wild-type enzyme (0.33 s^{-1}), at identical conditions of 50 μM nicotinamide and 500 μM NAD$^+$ (Table II). These results suggest that His-135 does not play a significant role in the nicotinamide exchange reaction (and thus nicotinamide-ribosyl cleavage) but is critical for a subsequent step in catalysis and the ultimate generation of 2′-*O*AADPr. As suggested, His-135 may act as a general base and activate the 2′-OH for nucleophilic attack on the C-1′ iminium intermediate (Scheme 1, model 2).

To test this hypothesis, the role of His-135 (HST2 number-

ing) during the nicotinamide-ribosyl cleavage step in the reaction was investigated by examining the ability of the H135A mutant to catalyze transglycosidation using nicotinamide and 2′-ribo-FNAD$^+$. If indeed His-135 functions to activate the 2′-OH for attack on the intermediate and plays only a minor role in nicotinamide-ribosyl cleavage, then histidine replacement should *not* produce an additional effect on the nicotinamide exchange rates with 2′-ribo-FNAD$^+$ because both alterations affect the same catalytic step in the same manner, by blocking acetyl transfer to the 2′-OH, after formation of the C1′ iminium adduct. Consequently, the difference in base-exchange rates between wt HST2 and H135A mutant with 2′-ribo-FNAD$^+$ should be similar to the differences observed between wt and mutant when using NAD$^+$ (~3-fold). By utilizing the identical conditions for nicotinamide exchange (see Table II for conditions and results), the difference (5.6-fold) in exchange rates between 2′-ribo-FNAD$^+$ and NAD$^+$ using H135A was only 2-fold lower when comparing the difference (3-fold) between and 2′-ribo-FNAD$^+$ and NAD$^+$ for wt enzyme. These results provide additional evidence that transglycosidation and acetyl group transfer to the 2′-OH are distinct, kinetically separable events and that His-135 and the 2′-OH of the nicotinamide ribose are not essential for the first step of the chemical mechanism, cleavage of the nicotinamide-ribosyl C—N bond.

TABLE II

Sir2-catalyzed nicotinamide exchange with 2′-ribo FNAD$^+$ and NAD$^+$

The first two rows represent apparent V_{max} values determined from initial exchange rates at nicotinamide concentrations ranging from 50 to 2000 μM. Reactions were carried out in PBS buffer, pH 7.3, at 37 °C, 300 μM acetylated H3 peptide, 1 mM DTT, and 500 μM NAD$^+$ or 1.91 mM 2′-ribo FNAD$^+$. Controls (without enzyme) at each nicotinamide concentration were subtracted from each raw rate to determine the enzyme-catalyzed rate. The complete data sets were then fitted to the Michaelis-Menten equation to obtain the apparent maximal exchange rate at fixed co-enzyme concentration. The bottom two rows represent exchange rates determined at fixed nicotinamide (50 μM), and either 500 μM NAD$^+$ or 800 μM 2′-ribo FNAD$^+$.

Sir2 homologue	Exchange rate β-NAD$^+$	Exchange rate β-dFNAD$^+$
	s^{-1}	
HST2	3.3 ± 0.2	0.016 ± 0.004
hSIRT2	2.4 ± 0.3	0.002 ± 0.0001
HST2[a]	0.33 ± 0.02	$2.3 \pm 0.1 \times 10^{-4}$
HST2-H135A[a]	0.12 ± 0.03	$4.1 \pm 0.3 \times 10^{-5}$

[a] Rates determined at 50 μM nicotinamide and 500 μM NAD$^+$ or 800 μM 2′-ribo FNAD$^+$

DISCUSSION

Mechanism of Nicotinamide Inhibition and Transglycosidation—Recent work (28, 30) has identified nicotinamide as a noncompetitive inhibitor of Sir2 activity with an IC_{50} value less than 50 μM (28). Bitterman *et al.* (28) have proposed that the noncompetitive inhibition observed with nicotinamide is the result of nicotinamide binding to an alternative site on the enzyme surface, in close proximity to the NAD$^+$ binding site. This alternative binding site is referred to as site C and has been described in several x-ray crystal structures of Sir2 homologues. However, nicotinamide has never been observed at this site. Alternatively, inhibition may stem from an efficient transglycosidation reaction catalyzed by Sir2 enzymes.

To evaluate these two mechanisms of nicotinamide inhibition, we first examined the relationship between nicotinamide exchange and inhibition by using yeast HST2 and human SIRT2. Fig. 1 clearly shows that nicotinamide exchange (transglycosidation) correlates with inhibition for both enzymes and that nicotinamide exchange is a saturable reaction with respect to nicotinamide levels. These results are consistent with inhibition resulting from interception of an enzyme-ADPr intermediate during the formation of *O*AADPr and deacetylated substrate. Moreover, the observation that increased nicotinamide concentrations do not inhibit the transglycosidation reactions argues against inhibition via an allosteric site. Although these results do not preclude slight inhibition due to binding of nicotinamide in a separate, inhibitory site, such interactions must play only a minor role in the observed inhibition.

Additional support for transglycosidation-mediated nicotin-

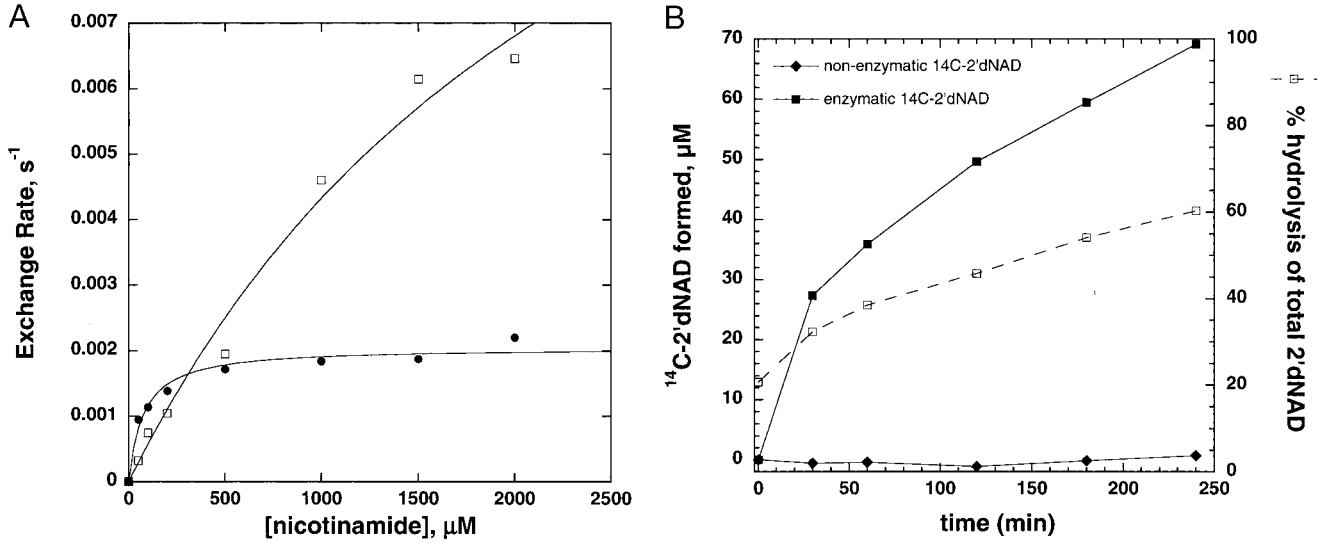

FIG. 5. *A*, initial rates of catalyzed nicotinamide exchange as a function of [nicotinamide] using 2′-ribo-FNAD$^+$ as coenzyme. Initial exchange rates at nicotinamide concentrations ranging from 50 to 2000 μM were carried out in PBS buffer, pH 7.3, 37 °C, 300 μM acetylated H3 peptide, 1 mM DTT, and 500 μM NAD$^+$ or 1.91 mM 2′-ribo-FNAD$^+$, and 7.8 μM hSIRT2 (*filled circles*) or 79 μM HST2 (*open squares*). Controls (without enzyme) at each nicotinamide concentration were subtracted from each raw rate to determine the enzyme-catalyzed rate. The complete data sets were then fitted to the Michaelis-Menten equation to obtain the apparent maximal exchange rate at fixed co-enzyme concentration (Table II). *B,* nicotinamide exchange reaction with 2′-deoxy-NAD$^+$. Enzymatic exchange of [^{14}C]nicotinamide into 2′-dNAD (*solid squares*), control with no peptide present (*solid diamonds*), and background hydrolysis of 2′-dNAD to 2′-dADPr (*open squares*, *right y* axis). 100-μl reactions consisted of 80 μM HST2, 500 μM 2′-dNAD, 500 μM AcH3, 1 mM DTT, 50 μM [^{14}C]nicotinamide, at 25 °C. Reactions were analyzed by HPLC and liquid scintillation counting to determine incorporation of [^{14}C]nicotinamide into 2′-dNAD. Peak integration was used to determine the ratio of 2′-dNAD to 2′-dADPr and the % hydrolysis.

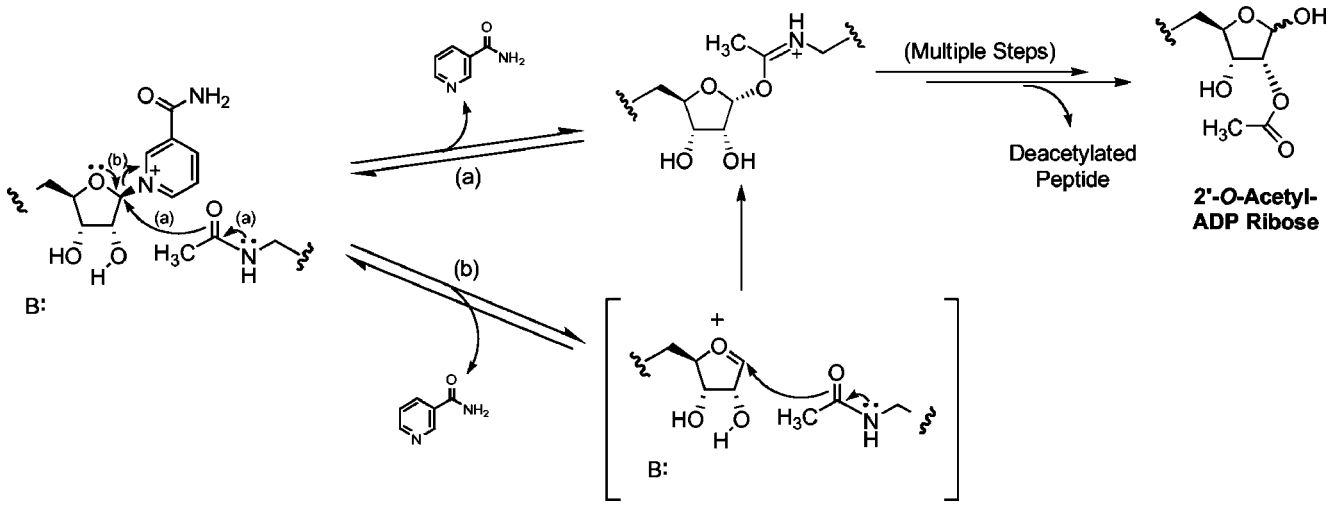

SCHEME 2. **Proposed mechanisms for the formation of 2′-*O*-acetyl-ADP-ribose from NAD$^+$ and acetylated substrate by the Sir2 enzymes.**

amide inhibition was obtained through the use of several pyridine/nicotinamide derivatives at C-3. Sir2-catalyzed transglycosidation in the presence of a variety of pyridine derivatives results in the ready formation of 3-substituted pyridine NAD$^+$ analogues. Although it is apparent that nucleophilicity of the exogenous base plays a role in how well the base acts as an inhibitor (Fig. 3*B*), and thus functions in transglycosidation, results from Table I indicate that binding contributions are also important. Thionicotinamide, which is the most structurally similar compound to nicotinamide, was found to be only a moderate inhibitor compared with nicotinamide. In general, the trends concerning inhibitory effects of the different pyridine derivatives are similar to those observed for bovine CD38-catalyzed transglycosidation (40), suggesting that the nucleophilicity of the base is the primary determinant of reactivity as long as minimal steric requirements are met. Furthermore, the Brönsted plot shown in Fig. 3*B* yielded a slope of +0.98, which shows that the dependence on basicity (pK_a of the nucleophilic base) is large, that the basicity is a good model for the transition state, and that there is a large amount of positive charge developed on the attacking nucleophile in the transition state for transglycosidation (41). It is interesting to note that nicotinamide is ~16-fold more efficient at transglycosidation than would be predicted from the Brönsted analysis of 3-substituted pyridines, indicating that nucleophilic selectivity by Sir2 enzymes is not solely dependent on basicity.

The transglycosidation reaction requires the cleavage of the nicotinamide-ribosyl bond to generate an enzyme-bound intermediate with release of the nicotinamide into solution. This intermediate must be sufficiently stable in order to react with exogenous nicotinamide or other 3-substituted pyridines to regenerate a pyridine nucleotide moiety. But unlike CD38 where solvolysis readily occurs in the absence of exogenous bases (42), the intermediate on Sir2 must be sequestered from water or solvent so that insignificant hydrolysis is observed, except under conditions where the enzyme-bound intermediate is denatured or reaction progress is blocked, *e.g.* by replacement of the 2′-OH by fluorine. Indeed, significant amounts of ADP-2′-F-ribose were detected during the nicotinamide exchange reaction with 2′-ribo-FNAD$^+$ (data not shown). Two likely transient species can be envisioned that would account for the transglycosidation reaction, either through the formation of a covalent enzyme-ADP-ribose intermediate or formation of a solvent-inaccessible high energy intermediate (such as formation of an imine between peptide and ADP-ribose, or a stabilized oxocarbenium ion) (Scheme 2).

In the reported crystal structures of Sir2 homologues, no active-site nucleophiles were found in proximity to the nicotinamide-ribosyl bond (24, 33, 39) with the exception of the conserved histidine residue in proximity to the C-3 hydroxyl group. A conserved serine residue within site C has been proposed as the nucleophile responsible for the cleavage of nicotinamide (33); however, it is difficult to rationalize the reactivity of the intermediate with formation of a glycosidic bond to a serine hydroxyl. Chang *et al.* (24) reported that mutation of this residue caused changes in the enzymatic activity that were consistent with only structural perturbations. Furthermore, attempts to trap such an enzyme intermediate have been negative using the HST2 mutant H135A and ^{32}P-labeled NAD$^+$ as substrate, where only background levels of radioactivity were observed (data not shown). What label was incorporated into protein was comparable with control reactions containing denatured enzyme, suggesting nonspecific reaction of a nucleophile on the enzyme surface with the furanosyl aldehyde sugar moiety present in either ^{32}P-labeled ADP-ribose or *O*AADPr (43).

Instead of a covalent ADP-ribose-enzyme intermediate, the initial step in the reaction likely involves a solvent-inaccessible high energy intermediate, which is formed through the elimination of nicotinamide (Scheme 2). There are several examples in the literature, which implicate the formation of an oxocarbenium ion during enzymatic catalysis for a variety of diverse enzymes (44–50). Most relevant to the Sir2 enzymes are the CD38/NAD$^+$ glycohydrolases and the ADP ribosyltransferases. Although an oxocarbenium ion-like intermediate was originally proposed for the CD38 enzymes (35, 51–55), there have been conflicting reports (37, 56) suggesting an obligatory involvement of anion stabilization of the transition state and subsequent formation of a covalent ADP-ribose/enzyme intermediate. A similar mechanism involving an anion-stabilized transition state was proposed for the ADP-ribosyltransferases (57). On the other hand, the absolute requirement of a carboxylate nucleophile or anionic stabilization for cleavage of the nicotinamide-ribosyl bond can be questioned in diphtheria toxin. Mutation of the only anion, Glu-148, positioned within 7 Å of the scissile bond to either serine or glutamine has little effect on the rate of NAD$^+$ hydrolysis (58). In contrast, the replacement of Glu-148 causes up to 300-fold decrease in the transferase activity, depending on the mutation (58); thus the anion appears to be involved in the transferase activity but not in the activation of the nicotinamide-ribosyl bond for cleavage.

In the Sir2 enzymes, Glu-45 (Sir2-Af1 numbering) is the only

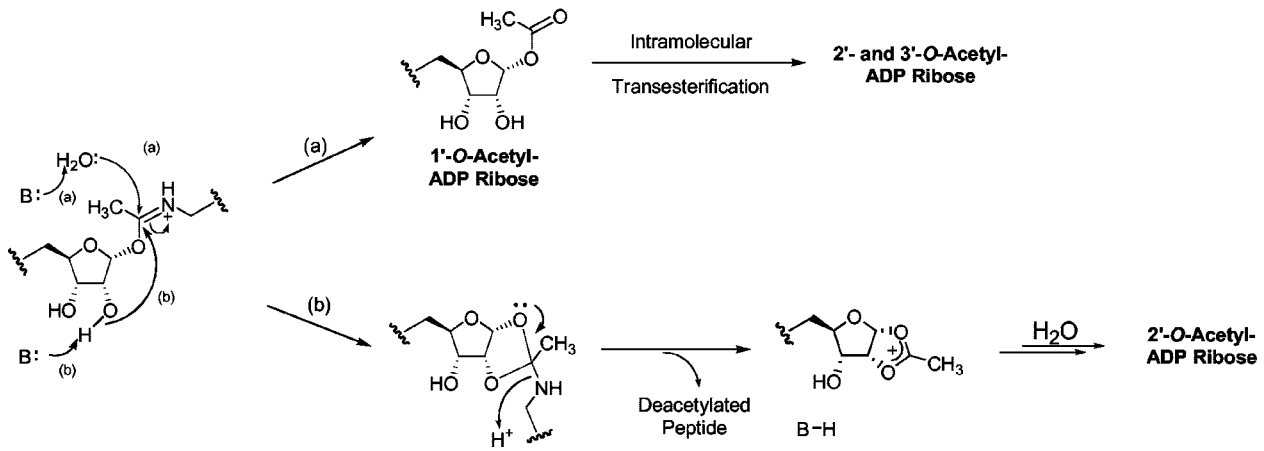

SCHEME 3. **Proposed mechanisms for the formation of 2′-*O*-acetyl-ADP-ribose starting from a proposed iminium ion intermediate.**

anionic residue within 10 Å of the nicotinamide-ribosyl bond. It should be noted, however, that in the reported crystal structure of Sir2Af1 co-crystallized with NAD^+ (33), the nicotinamide moiety was not observed and was modeled into the crystal structure. There are no other anionic or nucleophilic residues in proximity to the glycosidic bond of NAD^+ (16, 24, 33) with the exception of the conserved histidine described in the current study. Moreover, mutation of Glu-45 to an alanine does not alter catalytic efficiency (24) nor is this glutamate conserved among all Sir2 homologues.

Therefore, direct stabilization of the transition state by a side chain carboxylate (or other anionic side chains) does not appear to be a likely source of glycosidic bond activation in Sir2-like enzyme catalysis. However, there are two factors that likely contribute substantially to promote cleavage of the nicotinamide-ribosyl bond, namely desolvation and oxocarbenium stabilization through the formation of the iminium adduct with the peptide acetyl group (Scheme 2). For NAD^+ glycohydrolases, it has been proposed that desolvation within the active site renders the nicotinamide ribosyl bond more labile than in solution due to the loss of the rate-retarding entropic effects of solvation rather than enthalpic factors of transition state stabilization in the active site (59–61). This mechanism predicts that the binding site should be considerably hydrophobic, and all indications are that this is the case for Sir2 enzymes (16, 24, 33). Thus, desolvation energy may provide a significant driving force for glycosidic bond cleavage. Because NAD^+ cleavage requires an acetylated substrate, *i.e.* no transglycosidation is observed in the absence of acetylated peptide, binding of peptide would be necessary to create a sufficiently hydrophobic cavity.

In addition, a resulting oxocarbenium-like transition state may be stabilized through interaction with the carbonyl oxygen of the attacking acetyl group of substrate, implying at least partial bond formation at C-1 in the transition state, and subsequent generation of the iminium adduct with the peptide acetyl group (Scheme 2). Formally, two models can be considered. In *pathway a* of Scheme 2, nicotinamide release is the result of direct nucleophilic attack of the carbonyl oxygen in an S_n2 fashion to form an imine intermediate between ADP-ribose and peptide/protein substrate. In *pathway b*, the initial formation of an oxocarbenium ion occurs, followed by condensation with the amide oxygen of the substrate to form an imine intermediate as shown in *pathway a*. In terms of the transglycosidation reactions reported in this study, free nicotinamide could bind and react with either a tightly bound oxocarbenium ion intermediate or an iminium C-1 adduct between an ADP-ribosyl and acetylated peptide. Either high energy intermediate would be capable of partitioning between transglycosidation when sufficient nicotinamide is present and acetyl-transfer to the 2′-OH of ribose during the normal deacetylation catalytic cycle (Scheme 2).

The Involvement of the 2′-Hydroxyl in Cleavage of the Nicotinamide-Ribosyl Bond and in Deacetylation—Replacement of the 2′-OH with fluorine in 2′-ribo-$FNAD^+$ provides a direct probe of the function of the 2′-hydroxyl in the reaction catalyzed by Sir2. With 2′-ribo-$FNAD^+$, we have shown that although the enzymes perform nicotinamide exchange in the presence of acetylated substrate, the exchange is not directly coupled to transfer of the acetyl group to the 2′-hydroxyl. However, the slower rates (~200-fold with HST2) of exchange, using 2′-ribo-$FNAD^+$ and $dNAD^+$ (compared with NAD^+), indicate that the 2′-OH is important for optimizing the transglycosidation reaction. It is important to note that the rates of transglycosidation observed in our assays depend not only on the concentrations of nicotinamide, co-enzyme, acetylated substrate, and their associated binding constants but also on the net rate of nicotinamide-ribosyl C—N bond cleavage and the net rate of re-forming the glycosidic bond with a new nicotinamide molecule. Although clearly the presence of the 2′-OH is important for yielding faster rates of transglycosidation, it is difficult to unequivocally discern the exact source of the slower exchange rates with 2′-ribo-$FNAD^+$ and $dNAD^+$. Nonetheless, the observation that 2′-ribo-$FNAD^+$ and $dNAD^+$ yielded similar rates suggests that the inductive effects caused by the presence of the fluorine substituent may not account for the majority of this difference, and thus the effect may not be chemical in nature. Alternatively, the 2′-OH may be required for optimal binding and co-enzyme orientation within the active site for efficient nicotinamide ribosyl cleavage and bond re-formation. Consistent with this idea and the predicted loss of hydrogen bond capacity at the 2′-position when fluorine or hydrogen is the substituent, we have calculated an apparent K_i for 2′-ribo-$FNAD^+$ of 590 ± 160 μM, which is ~10-fold higher than the K_d reported for NAD^+ using Sir2Af2 (24), and is ~100-fold higher than the apparent K_m for NAD^+ determined with HST2.[2] Due to practical limitations, we were unable to use [2′-ribo-$FNAD^+$] higher than 0.8–1.9 mM and determine an accurate K_m.

Nicotinamide exchange reactions using the HST2 mutant H135A indicate that His-135 is not required for transglycosidation. H135A is catalytically impaired with respect to *O*AADPr formation, but the nicotinamide exchange rate is not appreciably affected. These data suggest that His-135 functions during the ultimate acetyl-transfer reaction to the 2′-OH, a conclusion consistent with the finding that the nicotinamide

exchange rate of H135A was similar with either 2′-ribo-FNAD$^+$ or NAD$^+$. The observation of a hydrogen bond network between this conserved histidine residue and the 3′-hydroxyl of ribose in the Sir2-Af1/NAD$^+$ crystal structure (33) suggests that His-135 may be indirectly involved in activating the 2′-hydroxyl for attack on the putative ADPr-acetyl peptide intermediate.

An important result from the utilization of 2′-ribo-FNAD$^+$ is the detection of a small but significant release of acetate when reactions are quenched under alkaline conditions (Fig. 4*A*, *bar 1*), suggesting that acetate is liberated from the hydrolysis of a labile enzyme intermediate. This species is likely 1′-*O*-acetyl-ADP-2′-deoxyfluororibose, formed directly by the enzyme or through the hydrolysis of the imine adduct at C-1′ to form 1′-*O*-acetyl-ADP-2′-deoxyfluororibose (Scheme 1, model 3). Subsequent hydrolysis of the C-1′ ester when quenched under alkaline conditions generates free acetate. The observation that ADP-2′-deoxyfluororibose is also formed during the pyridine exchange reactions with 2′-ribo-FNAD$^+$ is consistent with a competing reaction in which a water molecule reacts with this labile intermediate. Because the acetyl group transfer step to the 2′-OH is impossible with 2′-ribo-FNAD$^+$, water can eventually access and react with the dead-end enzyme/ADP-2′-F-ribose/acetyl-peptide intermediate. As mentioned, these results do not preclude formation of a tightly bound 1′-*O*-acetyl-ADP-2′-deoxyfluororibose as a stalled reaction intermediate, which could also liberate free acetate under hydrolytic conditions.

The HST2-catalyzed liberation of acetate using 2′-ribo-FNAD$^+$ supports a mechanism with NAD$^+$ where after nicotinamide-ribosyl cleavage, the carbonyl oxygen of acetylated substrate attacks the C-1′ ribose to form an imine adduct as illustrated in Scheme 1 (model 3). Once the iminium ion is generated, it could proceed through two distinct pathways to ultimately form 2′-*O*AADPr, both of which depend on the presence and activation of the ADPr 2′-OH, which may be facilitated by the conserved histidine residue (Scheme 3). In *pathway a* of Scheme 3, the iminium ion intermediate is first hydrolyzed to form 1′-*O*AADPr and subsequent intramolecular transesterification to generate 2′- and 3′-*O*AADPr. *Pathway b* of Scheme 3 proposes the formation of two different cyclized intermediates, which could ultimately form 2′-*O*AADPr. In the latter pathway, a water molecule attacks after the formation of a 1′-2′-cyclic acetoxonium intermediate (62, 63). Future studies will be directed at differentiating these two mechanisms.

The observed binding and activity of the 2′-ribo-FNAD$^+$ is in marked contrast to the reported properties of the corresponding arabino derivative. The 2′-deoxy-2′-fluoro-arabino-NAD$^+$ is a potent, slow-binding general inhibitor of CD38 (35). Although there is no evidence for formation of covalent intermediates with bovine CD38 using a range of 2′-substituted arabino-NAD$^+$ analogues (36), the mononucleotide, arabino-F-NMN$^+$, reportedly forms a covalent intermediate with CD38 (56). Interestingly, 2′-deoxy-2′-fluoro-arabino-NAD$^+$ has been reported by Sauve *et al.* (23) to be neither a substrate nor an inhibitor of Sir2 enzymes. This observation would imply that Sir2 is extremely sensitive to the stereochemistry at the 2′-position, *i.e.* 2′-deoxy-2′-fluoro-arabino-NAD$^+$ does not bind in the active site of Sir2 whereas 2′-ribo-FNAD$^+$ both binds and functions in the transglycosidation reaction.

While this manuscript was being reviewed, a study exploring the mechanism of nicotinamide inhibition was published (64). The general conclusions concerning the nature of the inhibition were similar to those presented in this paper.

Cellular Implications—The nature of Sir2 enzyme inhibition by nicotinamide is uniquely tied into the catalytic mechanism and therefore is a general feature of all Sir2 family members. Nicotinamide captures a reactive intermediate formed through the obligatory formation of an initial ternary complex between NAD$^+$, acetylated substrate, and enzyme. The net result is a block in deacetylation and the regeneration of NAD$^+$. Given this unique catalytic mechanism, the Sir2 reaction intermediate could act as a sensor of local nicotinamide levels that, when altered, would greatly influence Sir2-dependent protein/histone deacetylation. At relatively low nicotinamide levels (~10–500 μM), the extent of inhibition and transglycosidation is substantial, indicating that these levels fall within the ranges (11–400 μM) reported from natural sources (28) and could therefore regulate Sir2-like enzyme function. Other enzymes and metabolic pathways that produce or regulate nicotinamide levels may also have a profound effect on Sir2 activity. Consistent with this idea, Anderson *et al.* (65) have reported recently that a highly regulated gene *PNC1* encoding a nicotinamidase regulates ySir2 by depleting cellular nicotinamide levels. It will be important to determine whether other potential candidate enzymes that generate nicotinamide (*e.g.* NAD$^+$ glycohydrolases, poly-ADP-ribose polymerases, and ADP ribosyltransferases) function as regulators of Sir2-like enzymes.

Acknowledgments—We thank Dr. Rolph Sternglanz (State College of New York, Stony Brook) for the generous sample of plasmid containing the HST2 mutant H135A. We also thank Brian Arbogast and Lilo Barofsky (Oregon State University) for mass spectral analysis of compounds described in this work.

REFERENCES

1. Kouzarides, T. (2000) *EMBO J.* **19,** 1176–1179
2. Roth, S. Y., Denu, J. M., and Allis, C. D. (2001) *Annu. Rev. Biochem.* **70,** 81–120
3. Grozinger, C. M., and Schreiber, S. L. (2002) *Chem. Biol.* **9,** 3–16
4. Moazed, D. (2001) *Curr. Opin. Cell Biol.* **13,** 232–238
5. Gasser, S. M., and Cockell, M. M. (2001) *Gene* (*Amst.*) **279,** 1–16
6. Denu, J. M. (2003) *Trends Biochem. Sci.* **28,** 41–48
7. Frye, R. A. (2000) *Biochem. Biophys. Res. Commun.* **273,** 793–798
8. Starai, V. J., Celic, I., Cole, R. N., Boeke, J. D., and Escalante-Semerena, J. C. (2002) *Science* **298,** 2390–2392
9. Starai, V. J., Takahashi, H., Boeke, J. D., and Escalante-Semerena, J. C. (2003) *Genetics* **163,** 545–555
10. Afshar, G., and Murnane, J. P. (1999) *Gene* (*Amst.*) **234,** 161–168
11. North, B. J., Marshall, B. L., Borra, M. T., Denu, J. M., and Verdin, E. (2003) *Mol. Cell* **11,** 437–444
12. Schwer, B., North, B. J., Frye, R. A., Ott, M., and Verdin, E. (2002) *J. Cell Biol.* **158,** 647–657
13. Onyango, P., Celic, I., McCaffery, J. M., Boeke, J. D., and Feinberg, A. P. (2002) *Proc. Natl. Acad. Sci. U. S. A.* **99,** 13653–13658
14. Vaziri, H., Dessain, S. K., Ng Eaton, E., Imai, S. I., Frye, R. A., Pandita, T. K., Guarente, L., and Weinberg, R. A. (2001) *Cell* **107,** 149–159
15. Luo, J., Nikolaev, A. Y., Imai, S., Chen, D., Su, F., Shiloh, A., Guarente, L., and Gu, W. (2001) *Cell* **107,** 137–148
16. Finnin, M. S., Donigian, J. R., Cohen, A., Richon, V. M., Rifkind, R. A., Marks, P. A., Breslow, R., and Pavletich, N. P. (1999) *Nature* **401,** 188–193
17. Smith, J. S., Brachmann, C. B., Celic, I., Kenna, M. A., Muhammad, S., Starai, V. J., Avalos, J. L., Escalante-Semerena, J. C., Grubmeyer, C., Wolberger, C., and Boeke, J. D. (2000) *Proc. Natl. Acad. Sci. U. S. A.* **97,** 6658–6663
18. Tanner, K. G., Landry, J., Sternglanz, R., and Denu, J. M. (2000) *Proc. Natl. Acad. Sci. U. S. A.* **97,** 14178–14182
19. Imai, S., Armstrong, C. M., Kaeberlein, M., and Guarente, L. (2000) *Nature* **403,** 795–800
20. Landry, J., Sutton, A., Tafrov, S. T., Heller, R. C., Stebbins, J., Pillus, L., and Sternglanz, R. (2000) *Proc. Natl. Acad. Sci. U. S. A.* **97,** 5807–5811
21. Tanny, J. C., and Moazed, D. (2001) *Proc. Natl. Acad. Sci. U. S. A.* **98,** 415–420
22. Jackson, M. D., and Denu, J. M. (2002) *J. Biol. Chem.* **277,** 18535–18544
23. Sauve, A. A., Celic, I., Avalos, J., Deng, H., Boeke, J. D., and Schramm, V. L. (2001) *Biochemistry* **40,** 15456–15463
24. Chang, J. H., Kim, H. C., Hwang, K. Y., Lee, J. W., Jackson, S. P., Bell, S. D., and Cho, Y. (2002) *J. Biol. Chem.* **277,** 34489–34498
25. Borra, M. T., O'Neill, F. J., Jackson, M. D., Marshall, B., Verdin, E., Foltz, K. R., and Denu, J. M. (2002) *J. Biol. Chem.* **277,** 12632–12641
26. Rafty, L. A., Schmidt, M. T., Perraud, A. L., Scharenberg, A. M., and Denu, J. M. (2002) *J. Biol. Chem.* **277,** 47114–47122
27. Anderson, R. M., Bitterman, K. J., Wood, J. G., Medvedik, O., Cohen, H., Lin, S. S., Manchester, J. K., Gordon, J. I., and Sinclair, D. A. (2002) *J. Biol. Chem.* **277,** 18881–18890
28. Bitterman, K. J., Anderson, R. M., Cohen, H. Y., Latorre-Esteves, M., and Sinclair, D. A. (2002) *J. Biol. Chem.* **277,** 45099–45107
29. Sandmeier, J. J., Celic, I., Boeke, J. D., and Smith, J. S. (2002) *Genetics* **160,** 877–889
30. Landry, J., Slama, J. T., and Sternglanz, R. (2000) *Biochem. Biophys. Res. Commun.* **278,** 685–690
31. Sleath, P. R., Handlon, A. L., and Oppenheimer, N. J. (1991) *J. Org. Chem.* **56,** 3608–3618
32. Bradford, M. M. (1976) *Anal. Biochem.* **72,** 248–254
33. Min, J., Landry, J., Sternglanz, R., and Xu, R. M. (2001) *Cell* **105,** 269–279

34. Zatman, L. J., Kaplan, N. O., and Colowick, S. P. (1953) *J. Biol. Chem.* **200,** 197–212
35. Muller-Steffner, H. M., Malver, O., Hosie, L., Oppenheimer, N. J., and Schuber, F. (1992) *J. Biol. Chem.* **267,** 9606–9611
36. Cakir-Kiefer, C., Muller-Steffner, H., Oppenheimer, N., and Schuber, F. (2001) *Biochem. J.* **358,** 399–406
37. Sauve, A. A., and Schramm, V. L. (2002) *Biochemistry* **41,** 8455–8463
38. Handlon, A. L., Xu, C., Muller-Steffner, H. M., Schuber, F., and Oppenheimer, N. J. (1994) *J. Am. Chem. Soc.* **116,** 12087–12088
39. Finnin, M. S., Donigian, J. R., and Pavletich, N. P. (2001) *Nat. Struct. Biol.* **8,** 621–625
40. Berthelier, V., Tixier, J. M., Muller-Steffner, H., Schuber, F., and Deterre, P. (1998) *Biochem. J.* **330,** 1383–1390
41. Jencks, W. P. (1987) *Catalysis in Chemistry and Enzymology*, pp. 79–85, Dover Publications, Inc., New York
42. Pascal, M., and Schuber, F. (1976) *FEBS Lett.* **66,** 107–109
43. McDonald, L. J., Wainschel, L. A., Oppenheimer, N. J., and Moss, J. (1992) *Biochemistry* **31,** 11881–11887
44. Zhang, Q., and Liu, H. (2001) *J. Am. Chem. Soc.* **123,** 6756–6766
45. Fedorov, A., Shi, W., Kicska, G., Fedorov, E., Tyler, P. C., Furneaux, R. H., Hanson, J. C., Gainsford, G. J., Larese, J. Z., Schramm, V. L., and Almo, S. C. (2001) *Biochemistry* **40,** 853–860
46. Werner, R. M., and Stivers, J. T. (2000) *Biochemistry* **39,** 14054–14064
47. Allart, B., Gatel, M., Guillerm, D., and Guillerm, G. (1998) *Eur. J. Biochem.* **256,** 155–162
48. Erion, M. D., Stoeckler, J. D., Guida, W. C., Walter, R. L., and Ealick, S. E. (1997) *Biochemistry* **36,** 11735–11748
49. Scheuring, J., and Schramm, V. L. (1997) *Biochemistry* **36,** 4526–4534
50. Scheuring, J., and Schramm, V. L. (1997) *Biochemistry* **36,** 8215–8223
51. Cakir-Kiefer, C., Muller-Steffner, H., and Schuber, F. (2000) *Biochem. J.* **349,** 203–210
52. Sauve, A. A., Munshi, C., Lee, H. C., and Schramm, V. L. (1998) *Biochemistry* **37,** 13239–13249
53. Muller-Steffner, H., Augustin, A., and Schuber, F. (1997) *Adv. Exp. Med. Biol.* **419,** 399–409
54. Muller-Steffner, H. M., Augustin, A., and Schuber, F. (1996) *J. Biol. Chem.* **271,** 23967–23972
55. Tarnus, C., Muller, H. M., and Schuber, F. (1988) *Bioog. Chem.* **16,** 38–51
56. Sauve, A. A., Deng, H., Angeletti, R. H., and Schramm, V. L. (2000) *J. Am. Chem. Soc.* **122,** 7855–7859
57. Berti, P. J., Blanke, S. R., and Schramm, V. L. (1997) *J. Am. Chem. Soc.* **119,** 12079–12088
58. Wilson, B. A., Reich, K. A., Weinstein, B. R., and Collier, R. J. (1990) *Biochemistry* **29,** 8643–8651
59. Buckley, N., Handlon, A. L., Maltby, D., Burlingame, A. L., and Oppenheimer, N. J. (1994) *J. Org. Chem.* **59,** 3609–3615
60. Buckley, N., Maltby, D., Burlingame, A. L., and Oppenheimer, N. J. (1996) *J. Org. Chem.* **61,** 2753–2762
61. Buckley, N., and Oppenheimer, N. J. (1996) *J. Org. Chem.* **61,** 7360–7372
62. Hilbert, G. E., and Johnson, T. B. (1930) *J. Am. Chem. Soc.* **52,** 4489–4494
63. Niedballa, U., and Vorbruggen, H. (1974) *J. Org. Chem.* **39,** 3654–3660
64. Sauve, A. A., and Schramm, V. L. (2003) *Biochemistry* **42,** 9249–9256
65. Anderson, R. M., Bitterman, K. J., Wood, J. G., Medvedik, O., and Sinclair, D. A. (2003) *Nature* **423,** 181–185